Different methods for physical and chemical elimination of strobilurin fungicides from wastewater

Ahmed I. Sheta (ahmed.sheta@acu.edu.eg)
Ahram Canadian University
Miriam F. Ayad
Ain Shams University
Amira M. El-Kosasy
Ain Shams University
Shereen M. Tawakkol
Helwan University
Ahmed S. Fayed
Cairo University

Research Article

Keywords: chitosan, alginate, MIR, MIP, photocatalyst, GO

Posted Date: February 11th, 2022

DOI: https://doi.org/10.21203/rs.3.rs-1336292/v1

Abstract

Molecular imprinting was developed as a method for selective adsorption. This makes molecular imprinting, a good option for elimination of different environmental interferents especially from wastewater. However, bio-polymeric adsorbents e.g. calcium alginate and chitosan-calcium alginate beads were used in wastewater treatment in different occasions, molecular imprints were found to be of superior elimination capacity than natural adsorbents. Conditions for optimum elimination were concluded to be 4 hrs shaking (150 rpm) at room temperature and pH 10 for 1 g alginate beads to eliminate 210 mg pesticide, pH 4 or 10 for 1 g chitosan-alginate beads to eliminate 480 and 1140 mg pesticide, respectively. However, with the same conditions at pH range 2-8, each gram of molecularly imprinted polymers (MIPs) could be used in elimination of 3290-3760 mg pesticide, and 1 g of molecularly imprinted resin (MIR) could eliminate 3280-3320 mg pesticide, which increased with increasing the shaking time to one day.

Also, resins, either alone or in combination with graphene oxide (GO) succeeded to act as a photocatalyst in chemical degradation of more than 65% of strobilurins under visible light, with high elimination capacity.

1. Introduction

Fungicides, like other pesticides, play a very important role in protection of different crops from many diseases caused by a wide variety of microorganisms. Although, the innovation of new molecules from natural origin, in order to eliminate or even reduce the environmental impact of toxic hazardous residues remaining after using these fungicides, they still have some toxicity on environment, and sometimes on human being e.g. kresoxim-methyl and pyraclostrobin cause a rapid raise in intracellular calcium and strong depolarization of mitochondrial membrane potential [1]{Regueiro, 2015 #1}{Regueiro, 2015 #1} {Noegrohati, 2018 #9}. The introduction of any contaminants affecting quality of water, is considered pollution [2]. {Regueiro, 2015 #1}Therefore, many efforts are needed to reduce and/or eliminate these toxic chemicals from environment safely as possible.

Strobilurin fungicides also when applied at environmentally relevant concentrations may cause mortality to larval and meta morph amphibians, however, chronic exposure effects in amphibians are still unclear [3].

Studies on strobilurins toxicity proved that low concentrations of azoxystrobin residues in the environment can be toxic to many aquatic animals, and invertebrates [4, 5]. Also showed that pyraclostrobin is potentially genotoxic and cytotoxic to human peripheral blood lymphocytes, neurotoxic to primary cultured
cutaneous neurons. This may interfere with some disorders in humans that may lead to autism and other neural diseases [6].

Although a relatively low toxicity has been claimed for this kind of compounds, information about their neurotoxicity is still scarce [1, 7, 8].

Regarding domestic animals and human being toxicity, kresoxim-methyl and pyraclostrobin were the most neurotoxic compounds causing a rapid raise in intracellular calcium [Ca^{2+}] and strong depolarization of mitochondrial membrane potential [1]. Also, it has been approved that strobilurins can decrease mitochondrial function and thus diminished growth and movement in zebrafish [9].

Wastewater treatment techniques are diverse and of different nature, chemical, biological, physical or combination of two or more techniques [2]. It is important to choose a technique with good elimination and regeneration properties. Polymeric adsorbents were used as a good candidate for physical elimination of pesticides.

Alginate is a natural polyelectrolyte extracted from seaweed, used in the form of sodium salt, to form hydrogel with water. Dropping of sodium alginate into calcium chloride, leads to its solidification in the form beads. These beads, bearing multiple charged sites (COO^-) available for electrostatic interaction with water soluble cations. In addition, the gel matrix formed with calcium, forms a good mesh for entrapping and adsorption of foreign materials in wastewater [10, 11].

Chitosan is a derivative of chitin, a natural polymer, used in the form of flakes, powder or hydrogel beads as a polymeric adsorbent. It is a linear polyelectrolyte that contains many (NH_3^+) groups at acidic pH. Thus, chitosan forms electrostatic complexes with alginate to build up a physically cross-linked three-dimensional matrix. Both, chitosan, and calcium-treated sodium alginate could be used alone or in combination with each other [11, 12].

Molecularly imprinted polymers (MIPs) were incorporated in sample preparation and concentration techniques, solid phase extraction methods and electrochemical sensors, due to selective recognition. They were better used for adsorption of molecules in organic solvents. However, molecularly imprinted resins (MIRs) were hydrophilic in nature with large number of amino, imino and hydroxyl groups for molecular binding in aqueous media [13].

Chitosan (CHS) and sodium alginate (ALG) are good examples of natural polymers that may be used in removal of hazardous materials from wastewater [11]. In comparison, molecularly imprinted polymers (MIPs) and resins (MIRs) were synthesized to play the same role with expected higher selectivity and better adsorption-regeneration properties.

Resorcinol-formaldehyde resins (MIR) have a visible-light photocatalytic activity that help in generation of hydrogen peroxide from water molecules [14]. Thus, they helped in chemical elimination of fungicides from wastewater. The addition of graphene oxide also helped more in catalytic photodegradation through enhancement of electron transfer [15].

2. Experimental

2.1. Chemicals and reagents

Azoxystrobin PESTANAL®, analytical standard; CAS Number: 131860-33-8 (AZX), pyraclostrobin PESTANAL®, analytical standard; CAS Number: 175013-18-0 (PYR), and trifloxystrobin PESTANAL®, analytical standard; CAS Number: 141517-21-7 (TRI) were purchased from Sigma-Aldrich®. Fungicide products, Amistar® (250 g/L), Bellis® (128 g/Kg), and Flint® (50%) were purchased from Syngenta, BASF, and BAYER companies' agent in Egypt. Chitosan (high molecular weight), ethylene glycol dimethacrylate (EGDMA), graphite powder, silica gel (60 for normal phase chromatography), HPLC grade acetonitrile and methanol were purchased from Sigma-Aldrich® (Germany). Acrylamide was obtained from Loba Chemie Pvt Ltd (India). Methacrylic acid (MA), hydrochloric acid (HCl), and sodium hydroxide (NaOH) were obtained from Oxford® (India). Glacial acetic acid (CH_3COOH), Phosphoric acid, potassium permanganate ($KMnO_4$), concentrated sulphuric acid (H_2SO_4), calcium chloride ($CaCl_2$), formaldehyde, resorcinol, urea, hydrogen peroxide (H_2O_2), and sodium alginate were purchased from Elgomhouria company, Egypt.

2.2. Apparatus

Jasco UV/VIS spectrophotometer (V630, Jasco Int. Co. Ltd, Japan), Jenway® pH meter (3505, Barloworld scientific ltd, UK), Unimax thermostatic shaker (IKA, Germany), a thermostatic multiple water bath (BT-15, Spain), IKA® magnetic stirrer (RH-basic 2) and thermometer. Shimadzu® IR Spirit Fourier transform infrared spectrophotometer (FTIR) was used for characterization.

Quanta 250 FEG (Field Emission Gun) scanning electron microscope (SEM) (FEI Company, USA) was used for surface imaging of MIPs, NIPs, MIRs and NIRs (10.1 mm working distance, with in-lens detector, and excitation voltage 20 kV).

Iron-dopped metal halide 400 W visible light lamp to simulate sunlight in photocatalytic degradation procedures.

2.3. Methods

2.3.1. Preparation of calcium alginate beads (ALG)

Sodium alginate (1.5 g) was dissolved in 100 mL distilled water and dropped by a plastic dropper into a beaker of 10% calcium chloride solution. The formed beads were then washed with distilled water, dried with oven at 60°C till solidification, and collected for use, after FTIR characterization [11].

2.3.2. Preparation of chitosan/calcium alginate beads (CHS/ALG)

High molecular weight chitosan (CHS, 1.5 g) was mixed with 5 mL acetic acid, and then distilled water was added to 100 mL. Sodium alginate (ALG, 1.5 g) was dissolved in 100 mL distilled water. Both components were mixed in a ratio (4 CHS: 1 ALG) for 1 hr using a magnetic stirrer and left to stand for 1 hr to obtain a bubble-free mixture. With a plastic dropper, CHS/ALG mixture was dropped in 10% NaOH, washed several times with distilled water till neutral pH and finally the beads were collected and added to 10% $CaCl_2$ till solidification. Beads were filtered and washed with distilled water then dried with oven at 60°C till solidification, collected for FTIR characterization, and used for adsorption [11].

2.3.3. Synthesis of molecularly imprinted polymers (MIPs)

Three monomers were used in construction of imprinted cage to bind and eliminate AZX selectively and efficiently. Acrylamide and hydroxypropyl β-cyclodextrin were mixed with methacrylic acid in equal ratio of (1.33: 1.33: 1.33 mM), in addition to 10 mM EGDMA cross linker and 0.15 mM benzoyl peroxide to initiate the polymerization reaction around the template of AZX 1 mM. Template, monomers, and cross linker were all mixed together in 5 mL porogenic solvent, acetonitrile, for 5 min under nitrogen, in a screw-capped glass test tube. In a 60°C thermostatically-controlled water bath, the sealed test tube was left over night for 24 hr, together with a blank test tube, without template, for synthesis of MIP and non-imprinted polymer (NIP), respectively [16].

Polymers (MIP, NIP) were collected, washed to remove unpolymerized materials and template, using a mixture of methanol and acetic acid (9: 1 v/v). The wash was scanned spectrophotometrically to ensure the cleanliness of the polymers. The powders were dried and characterized by FTIR and SEM.

2.3.4. Synthesis of molecularly imprinted resin (MIR)

Synthesis of superhydrophilic molecularly imprinted resin (MIR) was taken from Zhou et. al. [13] with some modifications. Silica gel beads were used as a core of solid support for the imprinted composite resin. Using one-pot condensation method, 0.45 mL formaldehyde was mixed with 0.33 g resorcinol in 30 mL distilled water for 1 hr at 40°C, using a magnetic stirrer, to form mixture I.

In another beaker, 0.23 mL formaldehyde and 0.126 g urea were mixed in 10 mL distilled water at 80°C till dissolve. Then, 0.35 g silica gel was mixed with 0.1 mL formaldehyde and the mixture was added to the beaker to form mixture II. All these components were ultrasonicated, and then added to mixture I. Template (i.e., pyraclostrobin or trifloxystrobin) (0.04 M solution in acetonitrile), was added in 10 mL volume to the whole mixture (I + II), left at 40°C/450 rpm/40 min, and finally the mixture was maintained at 80°C for 16 hrs. The resin was collected and washed thoroughly with methanol/acetic acid/distilled water (3/1/1) mixture, till no peaks detected spectrophotometrically. Another procedure was done for synthesis of non-imprinted resin (NIR), and both MIR and NIR were dried, characterized by FTIR and SEM then kept for use.

2.3.5. Synthesis of graphene oxide (GO)

Graphene oxide was synthesized according to the method mentioned in [17]. Three grams of graphite powder and 18 g $KMnO_4$ were added gradually and successively to a 9:1 mixture of concentrated H_2SO_4/H_3PO_4 (360:40 mL) with stirring at room temperature in open-mouthed flask. Then, the temperature was raised to 50°C with stirring for 18 h. After cooling to room temperature, the mixture was poured onto 400 mL ice with addition of 30 mL H_2O_2 and slightly stirred with glass bar. The mixture was centrifuged (5000 rpm for 5 min), and the sediment was collected and washed 7 times with 1 L 5% HCl solution each time, and further repeatedly with bi-distilled water (7 times, 1 L each time) until pH of the supernatant solution approached 7. After washing, the mixture was centrifuged (5000 rpm for 5 min), and the supernatant was discarded. The paste-like product was collected and dried at 60°C under constant vacuum for 2

days. The dried sample was ground, and sent for characterization using X-ray diffraction, FTIR and particle size measurement using TEM, to be used in other procedures.

2.3.6. Elimination procedures

A weighed amount of 0.1 g from CA, CHS/ALG and MIP adsorbents were added separately to bottle sets containing certain volume of AZX stock solution in acetonitrile diluted with distilled water of pH adjusted with NaOH and HCl. Another set of bottles were prepared in the same way using MIR as adsorbent and PYR as pesticide. The four sets were shaken at 150 rpm at room temperature. A sample was collected and filtered at zero time and after different time intervals to be measured spectrophotometrically for detection of AZX or PYR in solution, to evaluate the degree of elimination by each adsorbent [11]. Blank experiment was performed to exclude the adsorption by glassware.

A group of three beakers were prepared as follows; beaker 1, TRI was added to distilled water together with 0.1 g MIR, beaker 2, 0.1 g GO was added to TRI and MIR, and beaker 3, TRI only as a control. These beakers were subjected to visible light (after 2 hrs stirring in dark for equilibrium) and stirred with magnetic stirrers to avoid coagulation of powders. A similar group of three beakers were kept in dark to cancel any other factors that may interfere with photodegradation.

The experiment was repeated three times to calculate the average amount eliminated per gram adsorbent under equilibrium conditions [11]:

$$Qe = \left(\frac{C0 - Ce}{m}\right)v$$

where (Q_e) is the capacity of elimination by adsorbent in (mg/g), *C0* and *Ce* are the initial and final concentration of AZX, PYR or TRI in (mg/L), *V* is the solution volume in (L) and *m* is the adsorbent mass in (g).

Another set of bottles were prepared as follows; AZX and NIP, AZX and MIR, PYR and NIR, PYR and MIP in the same way as mentioned above at pH 6. Capacity of elimination was calculated for each bottle to be used in evaluation of imprinting together with selectivity of MIP and MIR [18]:

$$IF = \frac{Qmir}{Qnir}$$

$$IF = \frac{Qmip}{Qnip}$$

where (*IF*) is the imprinting factor that measure the magnitude of successful imprinting when its value is above unity.

$$\alpha = \frac{Qanalyte}{Qanalogue}$$

where (α) is the selectivity factor that reflects the selectivity of imprints to the analyte of interest.

2.3.7. Evaluation procedures

Stock solutions of AZX, PYR and TRI were prepared in concentration 10 mg/ 100 mL acetonitrile and refrigerated for working standards preparation. Calibration curves were constructed by scanning a serial dilution set of AZX, PYR and TRI, spectrophotometrically, at wavelength λ_{max} 245, 275 and 250 nm respectively.

This procedure helped in evaluation of washing step, in synthesis of MIP and MIR, and extent of elimination (Q_e).

2.3.8. Application on real wastewater samples

A volume of 5 mL Amistar® was diluted to 100 mL water, and the other fungicides were prepared by dissolving 10 g of Bellis® and Flint® in 100 mL water for each. All fungicides were applied on a field (175 m^2) of cucumber in different intervals. After irrigation, different samples of wastewater drained were collected. Samples were filtered by filter paper and measured spectrophotometrically. Further dilutions may be needed to reach concentrations relevant to the linearity ranges of AZX (2.5-20 µg/mL), PYR (3-20 µg/mL) and TRI (3-25 µg/mL). Samples pH was measured to help in choosing the proper adsorbent. Adsorbents were added in 0.1 g for AZX and PYR. However, in case of TRI samples, 0.1 gm MIR was added to two beakers in addition to 0.1 gm GO in one of them. Zero readings were recorded, then elimination procedures were applied. Samples were measured spectrophotometrically to evaluate the elimination efficiency.

3. Results And Discussion

3.1 Characterization of adsorbents

Functional group analysis was studied by fourier transform infrared analysis (FTIR) for CA beads, CHS/ALG beads, MIPs, MIRs and their initial components, showed the disappearance of initials and formation of new product with different properties, because of functional group changes, figures (1, 2 and 3). It was noticed that both imprinted and nonimprinted polymers have similar peaks, with those of nonimprinted more intense due to the absence of any self-assembly and random distribution of functional monomers without any cavity formation as in imprinted ones [18].

Surface morphology was studied for both molecularly imprinted polymers and resins (together with their nonimprinted powders).

Molecularly imprinted polymers (figure 4) showed formation of cavities in the polymerization process in presence of AZX template (figure 4, a), however, in absence of it, no cavities were constructed (figure 4, b).

Molecularly imprinted resin SEM images showed the large particle size due to the presence of silica gel core. However, these particles were smaller in MIR (figure 5, a) than in NIR (figure 5, b), due to the imprinting reaction that allowed resin to be arranged around template molecules.

The XRD pattern of graphene oxide (GO) showed two peaks at angles 11.079°θ (67.8 count) and 42.56°θ (25.1 count), together with the fingerprint region of FTIR were confirmed its formation (figure 6).

3.2 Optimization of elimination conditions

Time and pH for optimum adsorption and hence elimination of some strobilurins, were studied. Effect of pH on elimination was studied over the pH range 4-11 for both alginate and chitosan/alginate beads as they dissolve in highly acidic solutions. For alginate beads, it was noticed that after 4 hrs of shaking in room temperature at pH 10, the capacity of elimination was 210 mg/g for AZX. However, chitosan/alginate beads showed elimination capacity of 480 and 1140 mg/g at pH 4 and 10, respectively. After one day, adsorption capacity was decreased.

Capacity of MIP to eliminate AZX from aqueous solutions ranging from pH 2 to 11, was studied. A great improvement in elimination capacity (3290-3760 mg/g) was proved at pH 2-8, after reaching equilibrium. Few traces of AZX were detected after one day of shaking, however it was almost diminished after shaking for two days with MIP. After days, the substrate remained bounded to MIP adsorbent, thus elimination capacity was maintained over a large period.

Regarding MIR, its capacity of PYR elimination was comparable to that of MIP at pH 2-8. After equilibrium, it reached (3280-3320 mg/g) by shaking for one day and only few traces of PYR were detected after the second day. No decrease in elimination capacity by time.

Figure 7 shows the effect of pH on elimination of AZX from aqueous solution. Azoxystrobin solubility (6 mg/L) in water, together with its behavior in binding with different types of adsorbents studied, showed that the adsorption mechanism depends on Van der Waals forces without any ionic interaction [11].

Molecularly imprinted resin also showed a great elimination of PYR pesticide, (figure 7), due to its superhydrophilic nature that helped much more in adsorption of PYR in aqueous medium.

For photocatalytic degradation, it was reported that MIR needed 18 hrs to activate photocatalysis of TRI (after equilibrium). This period was reduced to 12 hrs after addition of GO that accelerated the chemical degradation process induced by the same visible light source under the same conditions of stirring and room temperature.

3.3 Evaluation procedures

The developed method for spectrophotometric analysis used in evaluation was characterized and validated in table 1.

Table 2 showed the calculated capacity of elimination (Qe) for the four types of adsorbents at different pH ranges, and for MIR alone and with GO. Also, imprinting factor (IF) and selectivity (α) were calculated for both imprints (MIP and MIR). It showed that the addition of chitosan to alginate, increases the solidification of calcium alginate to form cavities ready for binding with adsorbate either in acidic or basic pH, in comparison with chitosan alone that works in basic pH only. In addition, more functional groups e.g. NH_2 were added to increase the binding capacity [11]. This explains the better elimination capacity by chitosan/alginate beads rather than alginate alone.

Table 2 also showed values of imprinting factor (IF) for MIP and MIR, that reflected the success of imprinting procedures in synthesis of them. Selectivity coefficient (α) was calculated and explained the higher selectivity of both MIR and MIP.

In case of MIP, the addition of hydroxypropyl β-cyclodextrin to other monomers, built up a cup-like cavity that form multiple inclusion complexes with AZX, thus improving its elimination from wastewater greater than alginate and even chitosan/alginate beads. Also MIP could withstand different ranges of acidic pH, in addition to stability of adsorbate binding with time. However, the presence of silica core in MIR particles, made them arranged in a bed that offered a large adsorption surface area and was easily filtered or even may be packed in a column for wastewater purification, if needed.

Molecularly imprinted resins (MIR) under visible light, forms centers for charge carriers that serve as electron acceptors in photocatalysis [15]. Addition of graphene oxide to MIR increased their ability for photocatalytic degradation of TRI in visible light, this was attributed to the enhancement of charge transfer driven by the honeycomb SP^2 network structure of GO [19].

All these advantages made the molecular imprinting technique superior in wastewater purification (physically or chemically) than natural adsorbents e.g., chitosan and alginate.

3.4 Application on real samples

As the measured pH of the real samples was neutral to slightly acidic, alginate and chitosan/alginate beads failed to eliminate AZX. However, MIP and MIR succeeded to eliminate AZX and PYR, with elimination capacity of 3600 mg/g and 3000 mg/g, respectively.

Molecularly imprinted resin helped in photodegradation of TRI in wastewater samples with elimination capacities of 5100.3 mg/g and 5200 mg/g after addition of GO, respectively.

4. Conclusion

The molecularly imprinting technique greatly enhanced the elimination extent of the different harmful fungicides. Both MIP and MIR worked over a wide pH range with higher adsorption that increased over time till three days where only trace amounts of adsorbates were detected. They also bound to the selected adsorbate with irreversible binding that needed thorough washing with other solvents to remove the pesticide from the cavity of adsorbent. Thus, MIP and MIR provided an excellent adsorbent in wastewater purification over natural adsorbents like chitosan and/or alginate.

Molecularly imprinted resins played an important role in chemical elimination of fungicides through photocatalytic degradation reaction that only needed sunlight. This degradation may also be accelerated by addition of semiconductor nanoparticles like graphene oxide.

References

1. Regueiro, J., et al., *Toxicity evaluation of new agricultural fungicides in primary cultured cortical neurons.* Environmental Research, 2015. **140**: p. 37-44.
2. Russo, T., et al., *Sustainable Removal of Contaminants by Biopolymers: A Novel Approach for Wastewater Treatment. Current State and Future Perspectives.* Processes, 2021. **9**(4): p. 719.
3. Hartman, E.A.H., et al., *Chronic effects of strobilurin fungicides on development, growth, and mortality of larval Great Plains toads (Bufo cognatus).* Ecotoxicology, 2014. **23**(3): p. 396-403.
4. Cui, F., et al., *Toxicity of three strobilurins (kresoxim-methyl, pyraclostrobin, and trifloxystrobin) on Daphnia magna.* 2017. **36**(1): p. 182-189.
5. Olsvik, P.A., et al., *Effects of the fungicide azoxystrobin on Atlantic salmon (Salmo salar L.) smolt.* Ecotoxicology and Environmental Safety, 2010. **73**(8): p. 1852-1861.
6. Han, Y., et al., *Integrated assessment of oxidative stress and DNA damage in earthworms (Eisenia fetida) exposed to azoxystrobin.* Ecotoxicology and Environmental Safety, 2014. **107**: p. 214-219.
7. Zhang, C., et al., *Ecotoxicology of strobilurin fungicides.* Science of The Total Environment, 2020. **742**: p. 140611.
8. Zubrod, J.P., et al., *Fungicides: An Overlooked Pesticide Class?* Environmental Science & Technology, 2019. **53**(7): p. 3347-3365.
9. Kumar, N., et al., *Developmental toxicity in embryo-larval zebrafish (Danio rerio) exposed to strobilurin fungicides (azoxystrobin and pyraclostrobin).* Chemosphere, 2020. **241**: p. 124980.
10. Ngah, W.S.W. and S. Fatinathan, *Pb(II) biosorption using chitosan and chitosan derivatives beads: Equilibrium, ion exchange and mechanism studies.* Journal of Environmental Sciences, 2010. **22**(3): p. 338-346.
11. Nadavala, S.K., et al., *Biosorption of phenol and o-chlorophenol from aqueous solutions on to chitosan–calcium alginate blended beads.* Journal of Hazardous Materials, 2009. **162**(1): p. 482-489.
12. Lawrie, G., et al., *Interactions between Alginate and Chitosan Biopolymers Characterized Using FTIR and XPS.* Biomacromolecules, 2007. **8**(8): p. 2533-2541.
13. Zhou, T., et al., *Preparation of magnetic superhydrophilic molecularly imprinted composite resin based on multi-walled carbon nanotubes to detect triazines in environmental water.* Chemical Engineering Journal, 2018. **334**: p. 2293-2302.
14. Shiraishi, Y., et al., *Polythiophene-Doped Resorcinol–Formaldehyde Resin Photocatalysts for Solar-to-Hydrogen Peroxide Energy Conversion.* Journal of the American Chemical Society, 2021. **143**(32): p. 12590-12599.
15. Zhang, G., et al., *Macro-mesoporous resorcinol–formaldehyde polymer resins as amorphous metal-free visible light photocatalysts.* Journal of Materials Chemistry A, 2015. **3**(30): p. 15413-15419.
16. Abdel-Ghany, M.F., L.A. Hussein, and N.F. El Azab, *Novel potentiometric sensors for the determination of the dinotefuran insecticide residue levels in cucumber and soil samples.* Talanta, 2017. **164**: p. 518-528.
17. Raghubanshi, H., et al., *Synthesis of graphene oxide and its application for the adsorption of Pb+2 from aqueous solution.* Journal of Industrial and Engineering Chemistry, 2017. **47**: p. 169-178.
18. Ndunda, E.N., *Molecularly imprinted polymers—A closer look at the control polymer used in determining the imprinting effect: A mini review.* Journal of Molecular Recognition, 2020. **33**(11): p. e2855.
19. Mondal, A., et al., *Boosting Photocatalytic Activity Using Reduced Graphene Oxide (RGO)/Semiconductor Nanocomposites: Issues and Future Scope.* ACS Omega, 2021. **6**(13): p. 8734-8743.

Tables

Table 1. Assay parameters and method validation for spectrophotometric methods for determination of AZX, PYR and TRI

Parameters	AZX	PYR	TRI
Range (µg/mL)	2.5 - 20	3 - 20	3 - 25
Mean ± SD	98.98 ± 1.99	99.34 ± 1.48	98.56 ± 1.55
Slope	0.0562	0.0729	0.0553
Intercept	-0.0144	-0.0007	0.0025
Correlation coefficient (r)	0.9999	0.9995	0.9998
Accuracy	100.86 ± 0.7	100.04 ± 0.56	100.56 ± 1.18
RSD%[a]	1.71	0.59	1.94
RSD%[b]	1.48	1.57	1.99
LOQ (µg/mL)	1.16	0.57	2.22
LOD (µg/mL)	0.38	0.19	0.73

[a] the intra-day and inter-day respectively (n = 3) relative standard deviation of concentrations (AZX; 3, 7, 15 µg/mL), (PYR; 5, 10, 20 µg/mL) and (TRI; 5, 8, 20 µg/mL)

Table 2. Capacity of elimination of different adsorbents at different pH ranges for AZX and PYR, degree of photodegradation of TRI by MIR and MIR/GO at neutral pH, imprinting factor and selectivity of MIP and MIR at neutral pH

pH	Qe										IF		α	
	Chitosan	CHS/ALG	MIP-AZX	NIP-AZX	MIR-PYR	NIR-PYR	MIP-PYR	MIR-AZX	MIR-TRI	MIR/GO	MIP	MIR	MIP	MIR
2			3610		3300									
4		480	3760		3320									
6			3290	355.2398	3300	2013.423	3355.705	1776.199	5225.2	5225.2	9.2614	1.639	0.9804	1.85
8			3420		3280									
10	210	1140	1600		350									
11			90		170									

Figures

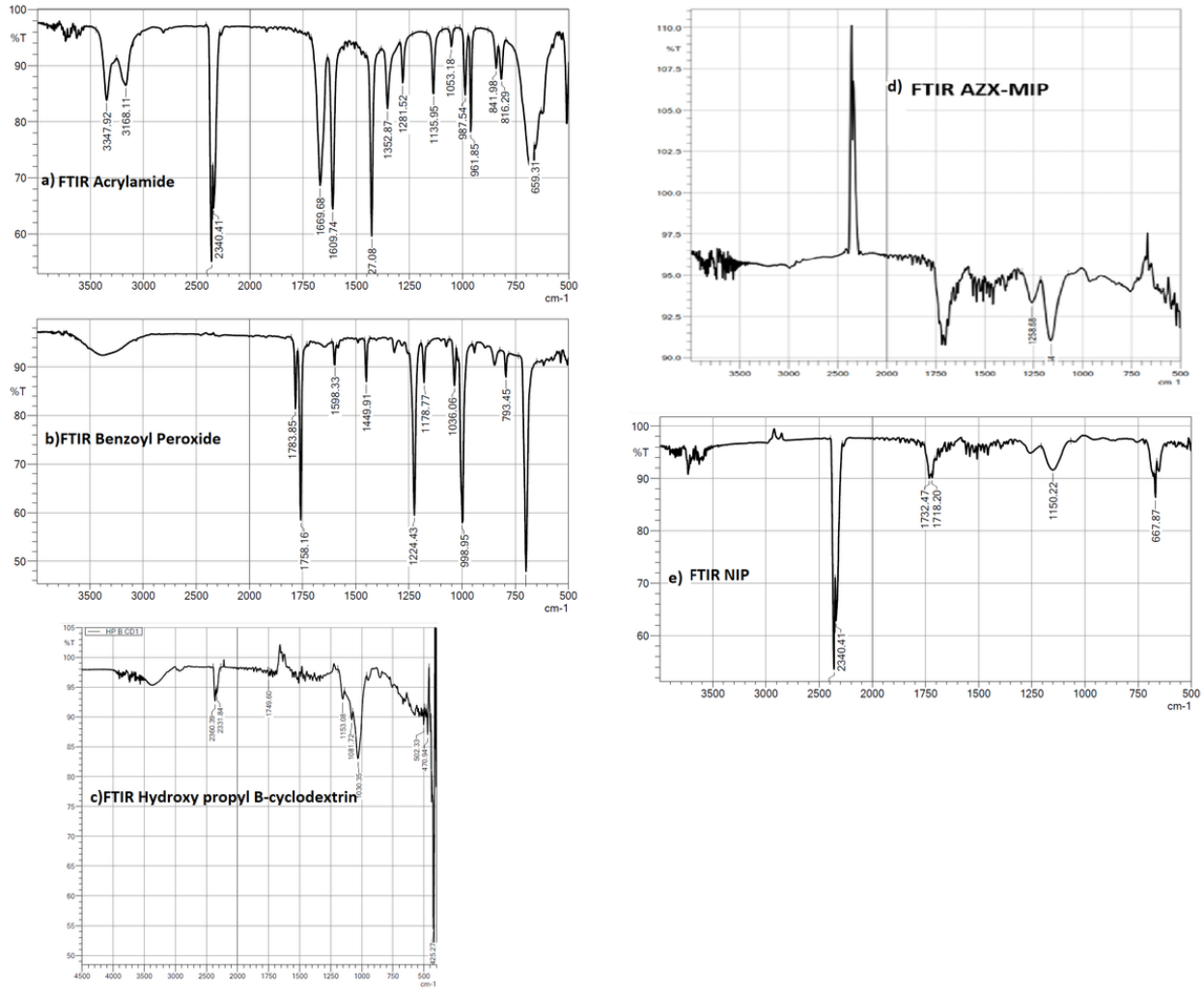

Figure 1

FTIR charts of MIP-AZX and its components together with NIP

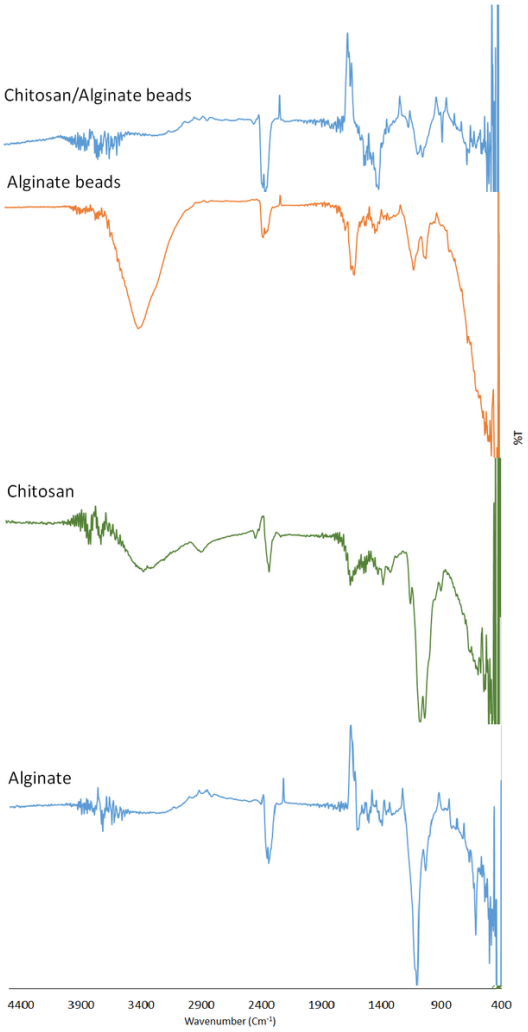

Figure 2

FTIR peaks of chitosan, alginate and their beads

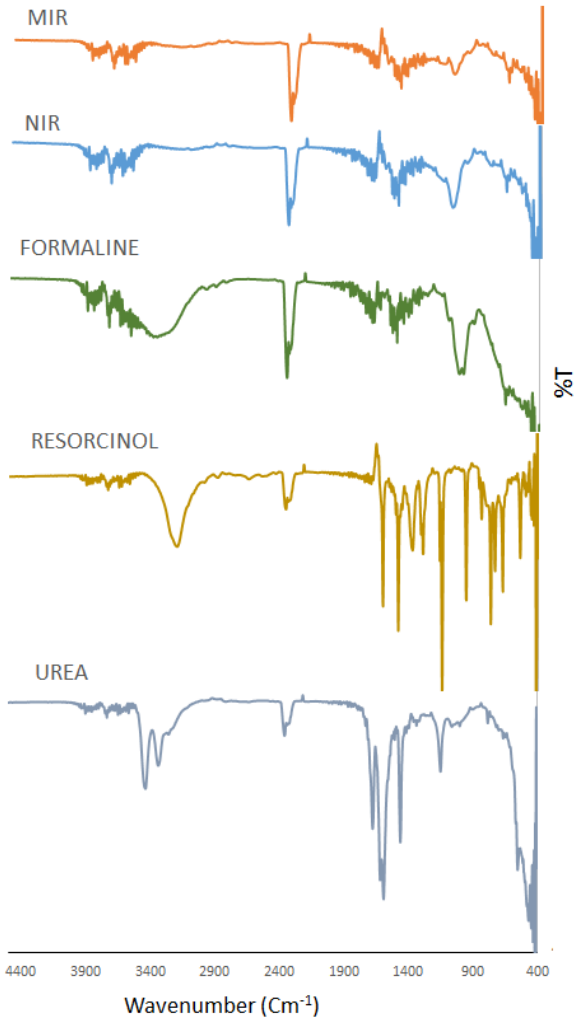

Figure 3

FTIR peaks of MIR and its components together with NIR

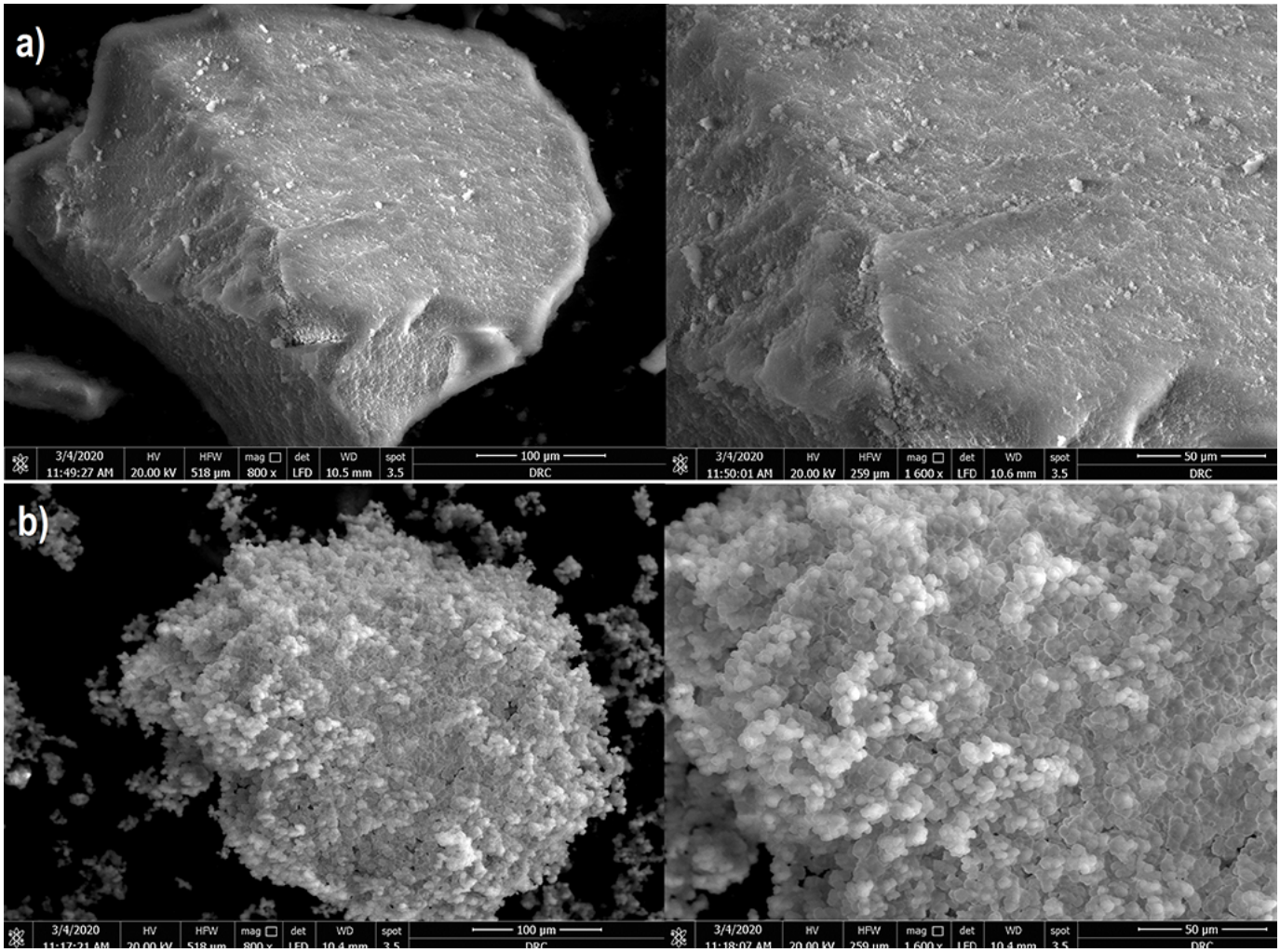

Figure 4

SEM images of MIP and NIP showing the difference in arrangement of formed cavities in MIP and solid surface in NIP

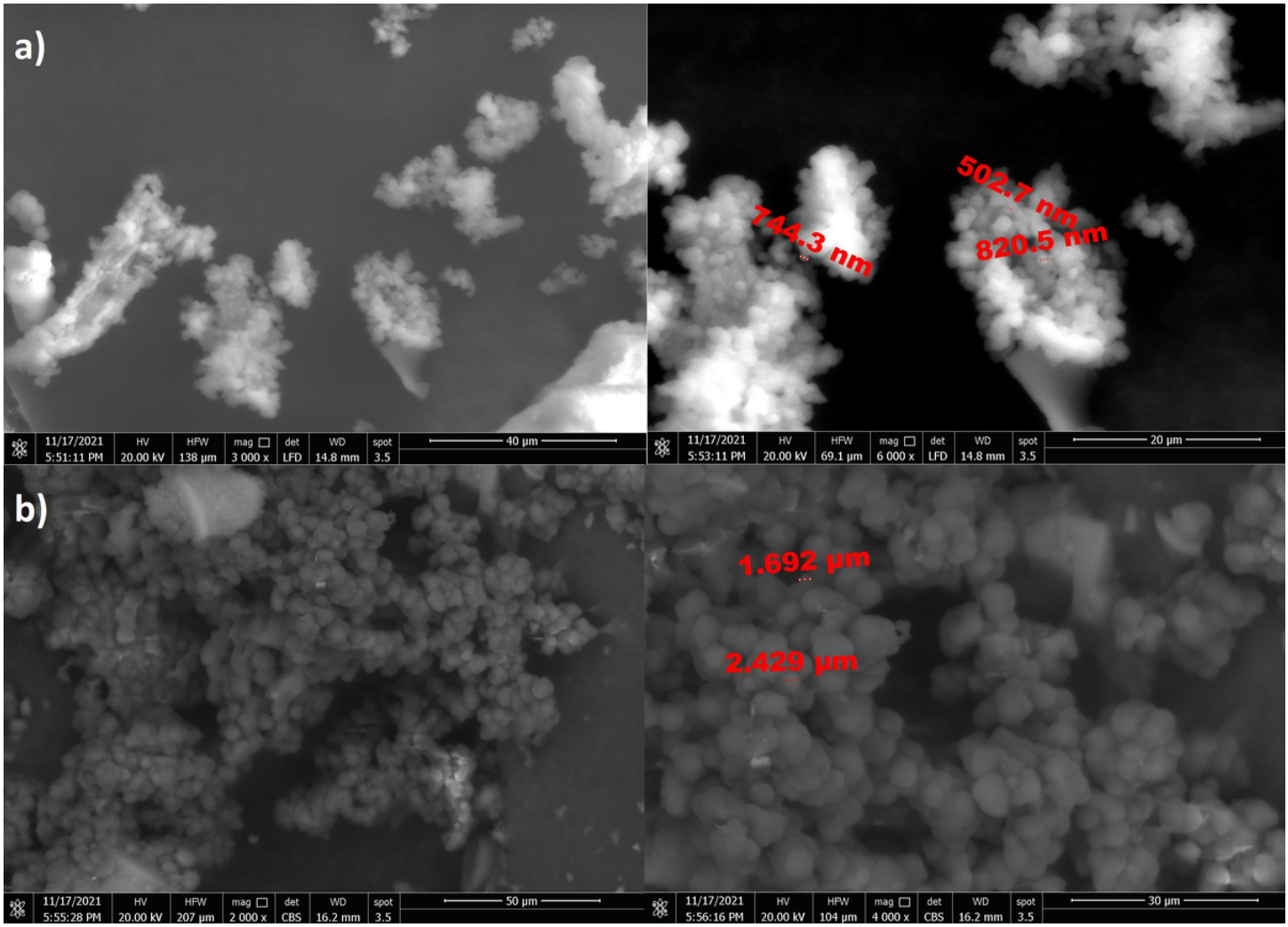

Figure 5

SEM images of MIR and NIR showing the difference in particle sizes as a result of arrangement of resin around template in MIR showing more cavities for binding

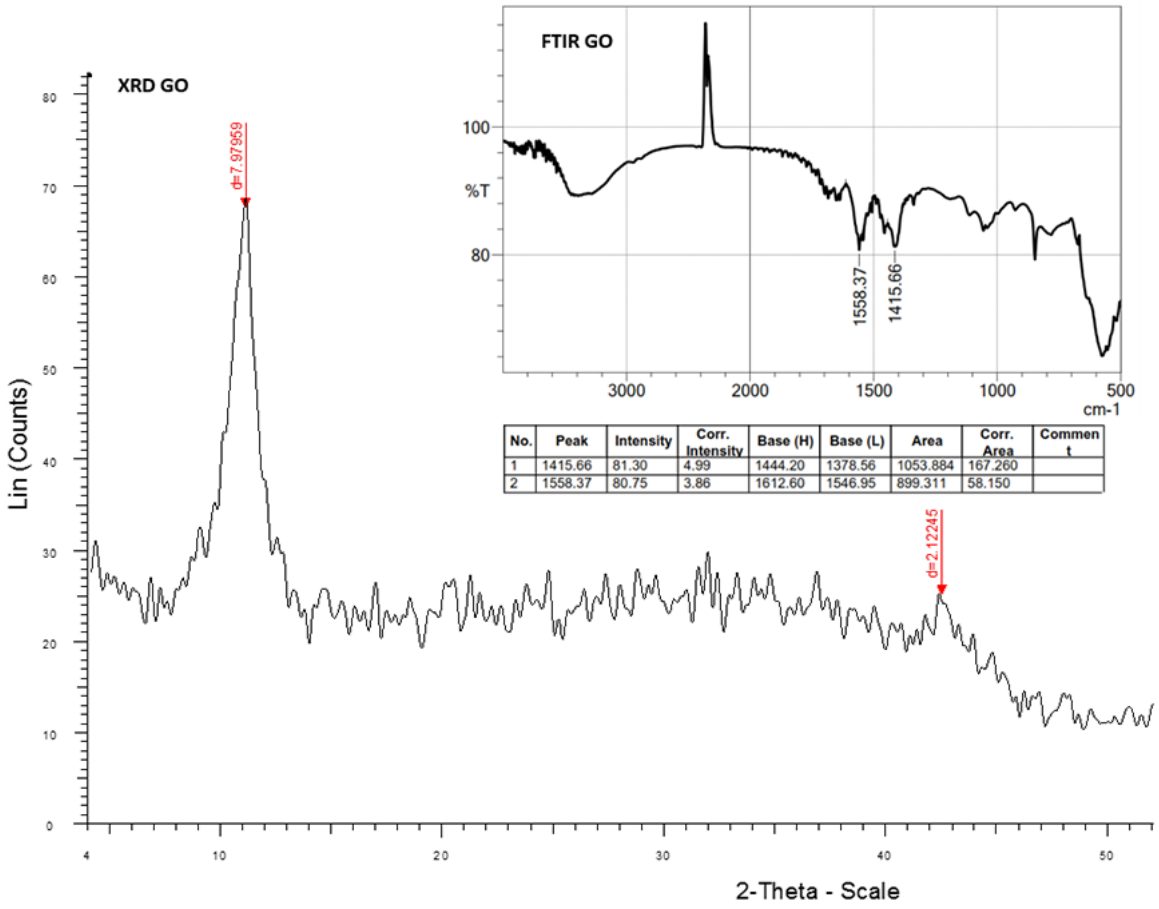

Figure 6

XRD and FTIR charts of graphene oxide (GO)

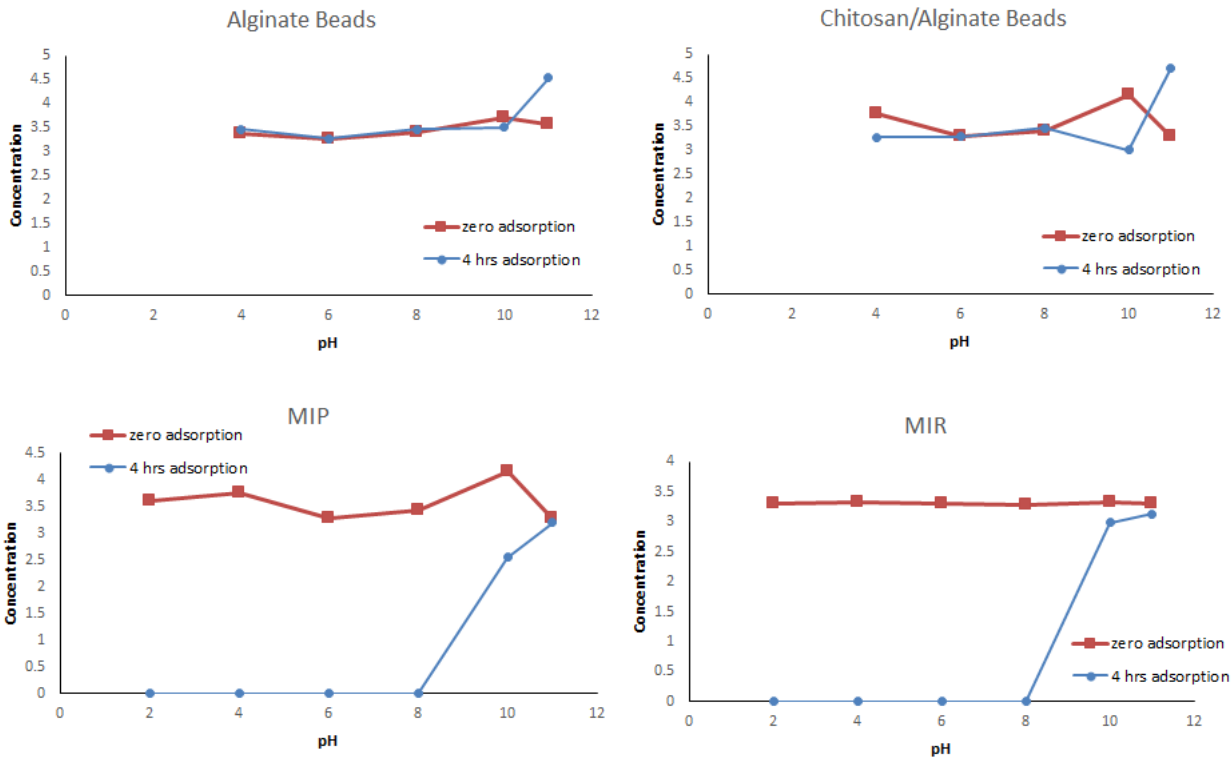

Figure 7

Adsorption profile for the four types of adsorbents over pH (2-11) at zero time and after 4 hrs